Simultaneous PET/MRI acquisition: Clinical potential in anatomically focused and whole-body examinations

Kathryn Fowler, MD, Jonathan McConathy, MD, PhD, Geetika Khanna, MD, Farrokh Dehdashti, MD, Tammie L.S. Benzinger, MD, PhD, Michelle Miller-Thomas, MD, Matthew Parsons, MD, Constantine Raptis, MD, Perry Grigsby, MD, Richard Laforest, PhD, Robert J. Gropler, MD, Vamsi Narra, MD, Barry A. Siegel, MD, John Kotyk, PhD, Agus Priatna, PhD, Robert McKinstry, MD, PhD, and Pamela K. Woodard, MD

The clinical availability of hybrid positron emission tomography (PET) and magnetic resonance imaging (MRI) systems offers medical imaging a range of potential benefits in oncologic, neurological, and cardiovascular applications.[1-5] One obvious benefit of simultaneous acquisition is improved image registration that allows optimal anatomic localization of PET findings. Other advantages include lower radiation dose in whole-body imaging compared with PET/CT (computed tomography), shorter overall imaging times, and the ability to simultaneously observe rapidly changing physiological and pathophysiological processes.

Drs. Fowler, McConathy, Khanna, Dehdashti, Benzinger, Miller-Thomas, Parsons, Raptis, Grigsby, Laforest, Gropler, Narra, Siegel, Kotyk, McKinstry, and Woodard practice at the Mallinckrodt Institute of Radiology and the Alvin J. Siteman Cancer Center, Washington University School of Medicine, St Louis, MO. Dr. Priatna is at R&D Collaborations, Siemens Healthcare, St Louis, MO.

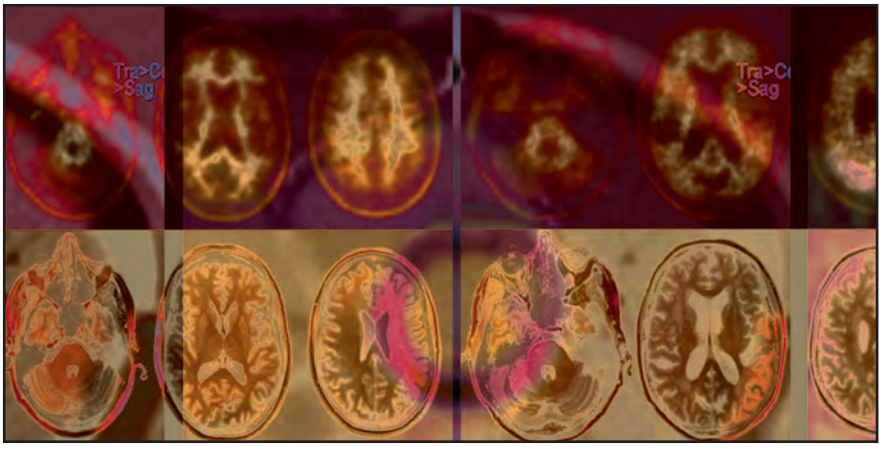

Most of the examples that follow are of patients scheduled for standard-of-care clinical fluorodeoxyglucose (FDG) PET/CT who, with Institutional Review Board (IRB) approval, were recruited for, and consented to undergo, additional PET/MR imaging. The simultaneous PET/MRI studies were acquired on a Biograph mMR system (Siemens Medical Systems, Erlangen, Germany) recently installed in the Center for Clinical Imaging Research (CCIR) at Washington University School of Medicine, St. Louis, MO. In this system, the PET component of the scanner with MR-compatible avalanche photodiodes (APDs) is present within the bore of a 3.0 tesla (T) magnet equipped with total imaging matrix and attenuation body-array and spine matrix coils.

Unlike PET/CT, PET/MRI uses a soft tissue, segmentation attenuation-correction (AC) μ-map. The AC μ-map was generated utilizing a dual-echo VIBE Dixon sequence that separates water and fat with TE1/TE2 = 1.23 msec/2.46 msec, TR = 3.6 msec, left-right FOV = 500 mm and anterior-posterior FOV = 300 mm.

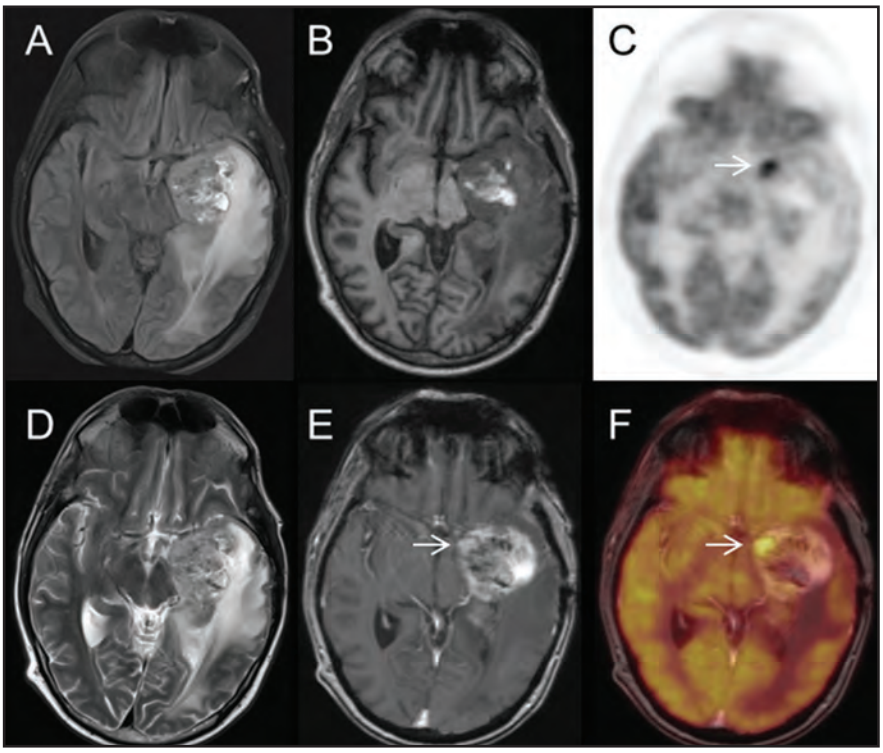

FIGURE 1. *Left temporal lobe primitive neuroectodermal tumor (PNET), recurrent after resection and radiation to the bed. Arrows show focal region of FDG uptake, which was found to be recurrent tumor and radiation necrosis. A = T2 FLAIR, B = T1 MPRAGE precontrast, C = FDG-PET, D = TSE T2, E = T1 postcontrast, F = fused FDG-PET and T1 postcontrast images.*

The acquisitions were performed either in a single station for dedicated PET/MRI or a multiple-station mode for whole-body imaging as indicated. Depending on the application, PET images were simultaneously acquired with the anatomical sequences from MRI, such as HASTE for whole-body acquisition, MPRAGE for brain imaging, SPACE or HASTE for pelvic applications, or delayed, contrast-enhanced, T1-weighted, phase-sensitive inversion-recovery imaging for cardiac imaging. Additional high-resolution MRI sequences were added for focused examinations; these included high-resolution T2 TSE, diffusion-weighted imaging (DWI) or diffusion-tensor imaging (DTI), and other sequences depending on the applications. Recent articles detail possible whole-body and dedicated protocols for oncologic imaging with PET/MR; however, the optimal sequences for workflow efficiency and diagnostic yield are yet to be determined in clinical practice.[6,7]

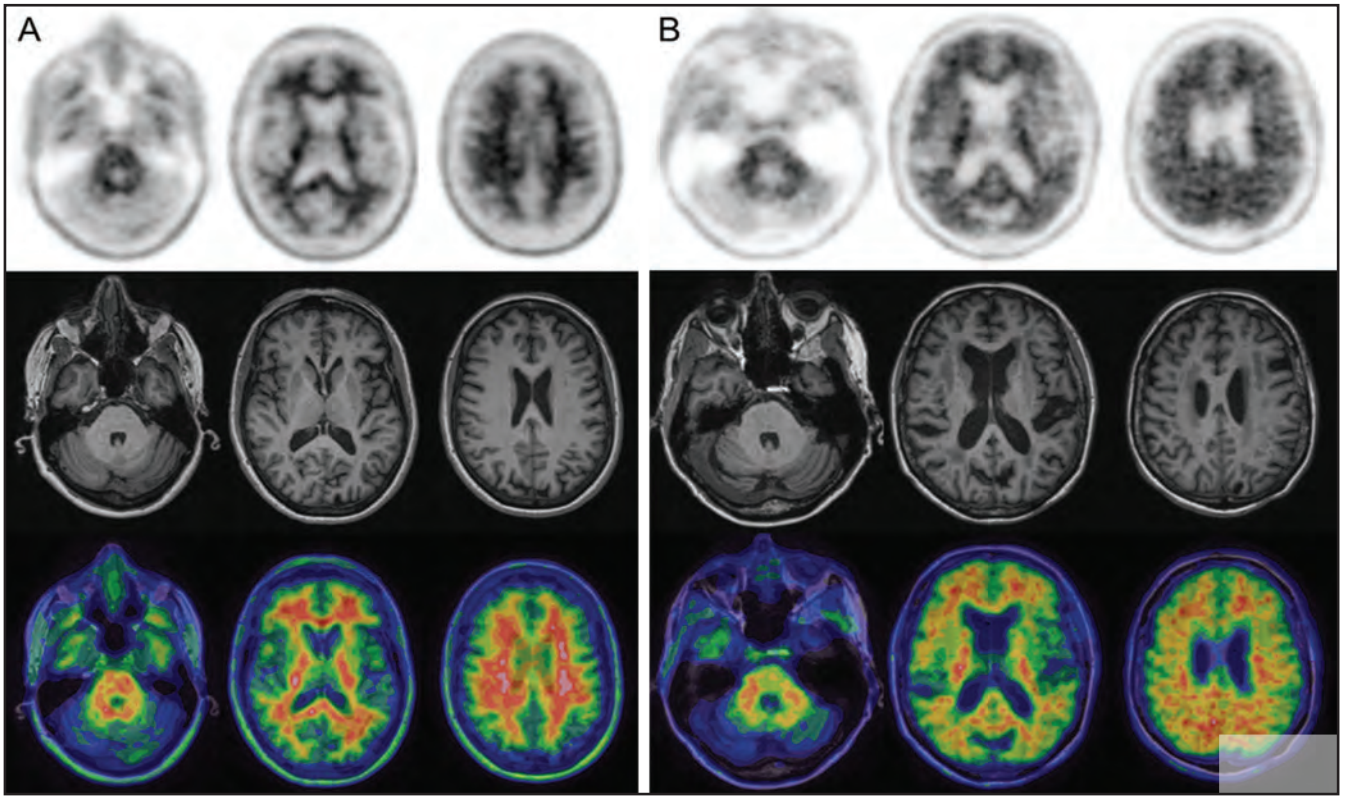

FIGURE 2. *Amyloid imaging with F-18 florbetapir. Panel A shows a normal control subject with no-to-sparse beta-amyloid plaques. Panel B shows a positive PET/MRI study, consistent with moderate to frequent beta-amyloid plaques.*

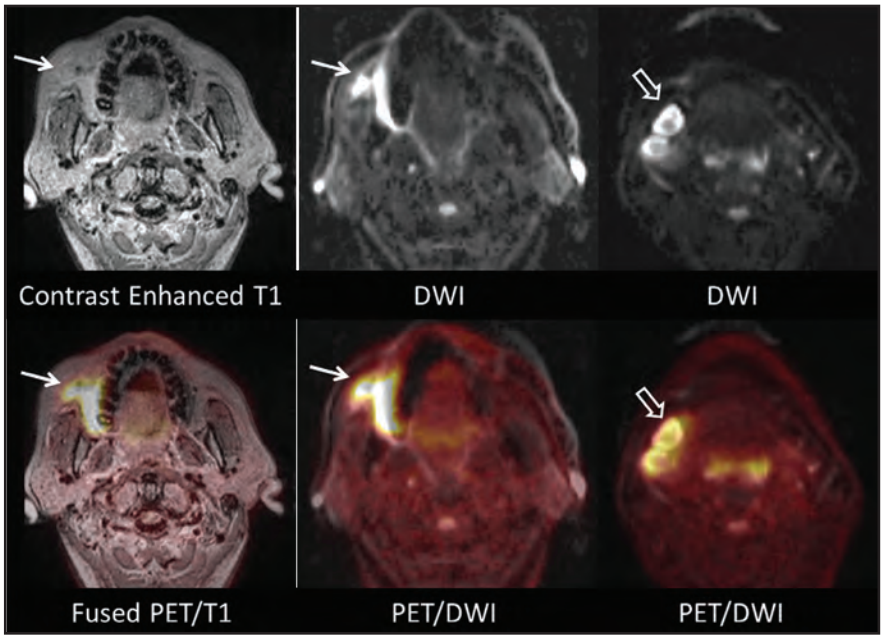

FIGURE 3. *Buccal cancer. Images depict a metabolically active tumor in the right buccal space (arrows), which also is well shown on the DWI and ADC map to restrict diffusion. The patient had biopsy-proven metastatic involvement of Ib lymph nodes within the right submandibular space (open arrows).*

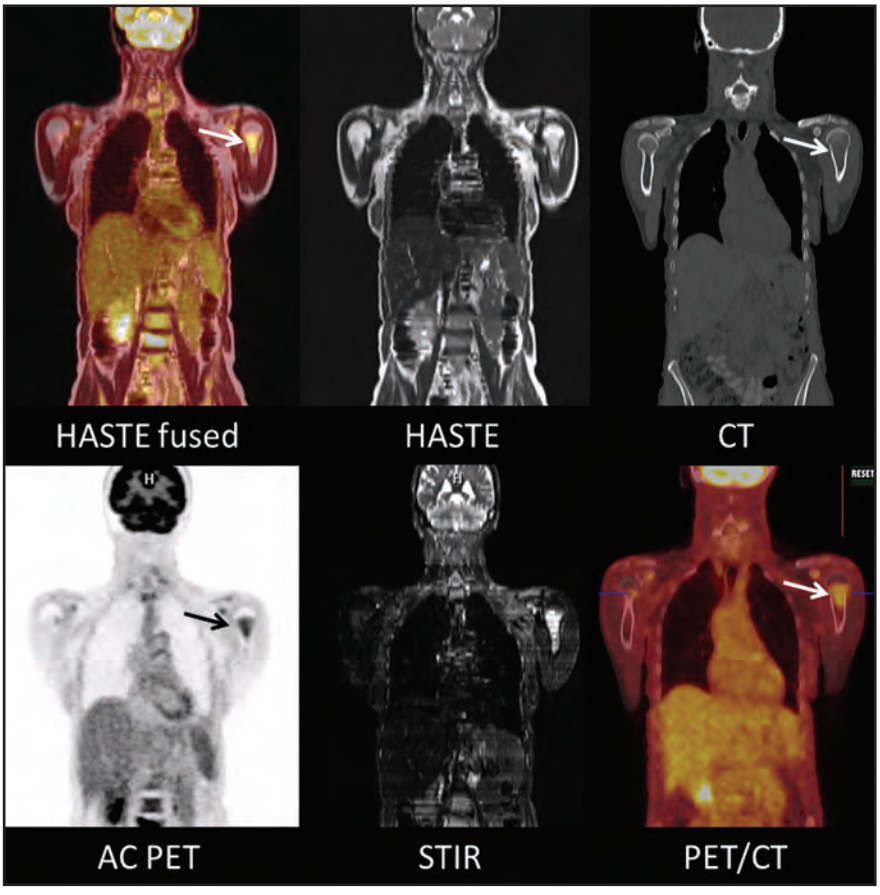

FIGURE 4. *Multiple myeloma. Images depict a focus of metabolically active disease in the left humeral neck that is more conspicuous on MRI than on CT alone (arrows).*

Clinical cases

The following are some examples of the clinically relevant cases acquired for anatomically focused and whole-body examinations with the Biograph mMR.

Neuro-oncologic brain imaging

While separately acquired brain MR and FDG-PET images can be fused through various software tools, a combined examination permits streamlined patient care and improves diagnostic specificity. The convenience and reduced burden to the patient of a single imaging session is particularly relevant to patients with brain tumors, who often have a reduced functional status.

Figure 1 displays a panel of selected simultaneous FDG-PET/MR images of a 41-year-old man with a left temporal lobe primitive neuroectodermal tumor (PNET) treated with near-total resection, craniospinal and resection-bed radiation therapy, and adjuvant chemotherapy. Follow-up MRI showed a growing, enhancing mass, and FDG-PET/MRI was performed to differentiate recurrent tumor from radiation necrosis. The white arrow denotes an enhancing nodule with markedly increased FDG uptake, highly suspicious for recurrent PNET. Subsequent surgical resection demonstrated a mixture of recurrent PNET and radiation necrosis.

Amyloid PET brain imaging

The development of F-18-labeled PET tracers for imaging beta-amyloid plaques that occur in Alzheimer's disease (AD) has the potential to increase the certainty of diagnosis in patients with cognitive impairment. One of these tracers, F-18 florbetapir, recently received FDA approval for clinical use, and several other amyloid PET tracers in late-phase clinical trials may soon become clinically available. If drugs that slow or reverse the development of AD dementia become clinically available, amyloid PET imaging may be a key component of patient selection for treatment and for monitoring response to therapy. The anatomic, volumetric, and functional data available through

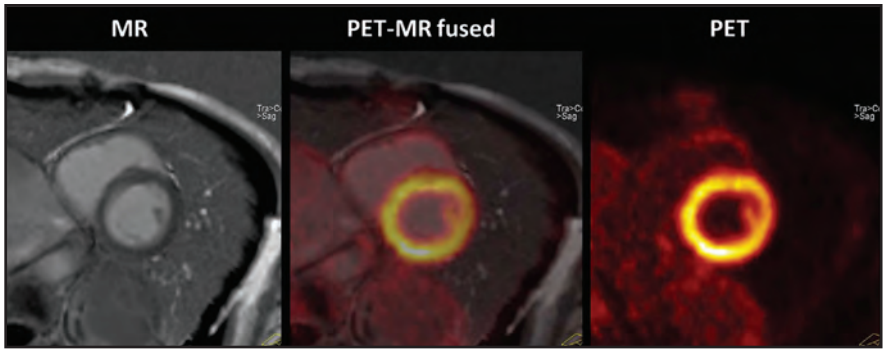

FIGURE 5. *Normal myocardial uptake. Simultaneous acquisition of ECG-gated PET and delayed contrast-enhanced (DCE) cardiac MR images (simultaneous acquisition of MR 2-point Dixon also acquired for attenuation correction prior to contrast injection). PET data were acquired in list mode and binned. DCE-MR images acquired in diastole are fused with diastolic PET data to create the center image.*

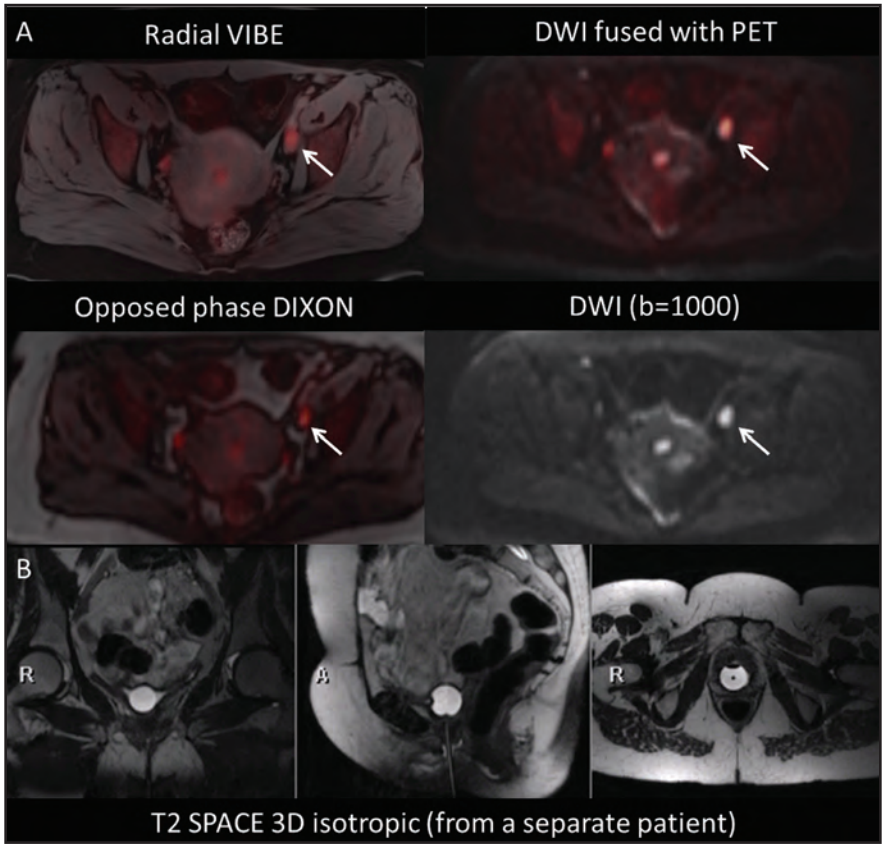

FIGURE 6. *Cervical cancer. Images (A) show a nodal metastasis in the left external-iliac chain (arrows) in a patient with cervical cancer. Additional images (B) from a separate patient demonstrate T2-SPACE sequence, 3D isotropic acquisition, which allows reformatted images to be constructed in multiple planes without loss of resolution.*

MRI can complement the biochemical information obtained through amyloid PET and provide a comprehensive, single-session neuroimaging evaluation of patients with cognitive impairment.

Figure 2 displays selected negative and positive F-18 florbetapir-PET/MR images from subjects enrolled in a research study. MRI provides excellent anatomic correlation for the localization of F-18 florbetapir accumulation in the white and gray matter and can also provide volumetric data for the detection of atrophy in regions like the hippocampus, which is often affected by AD. Clinical interpretation of F-18 florbetapir-PET relies primarily upon assessment of gray-white differentiation, with negative studies showing higher activity in the white matter than in the cerebral cortex (Figure 2) and positive studies showing loss of gray-white contrast due to the tracer binding to beta-amyloid plaques in the cerebral cortex (Figure 2).

Head and neck oncology

Simultaneous head and neck PET/MRI performs well compared with PET/CT in our initial experience. In the head and neck, PET/MRI combines the metabolic information from FDG-PET with high spatial resolution, anatomic localization, and soft-tissue contrast from MRI. MRI demonstrates better soft-tissue contrast than CT, permitting detection of perineural spread. Software fusion of PET and MRI data is challenging in the neck, and the simultaneous acquisition of the MRI and PET data provides improved coregistration.

Figure 3 illustrates images of a 58-year-old man with a recent diagnosis of squamous cell carcinoma of the right buccal space and metastatic involvement of right submandibular lymph nodes. Contrast-enhanced MRI shows excellent anatomic detail, and diffusion-weighted images demonstrate high contrast between the lymph nodes and adjacent fat in the submandibular space, which correlate to the areas of increased FDG uptake.

Multiple myeloma and bone imaging

The combination of functional and morphologic MRI sequences with PET imaging is of potential value in the evaluation of osseous metastases and primary bone neoplasms, such as multiple myeloma. DWI, T2 fat-suppressed sequences, and T1-TSE images can all depict bone lesions that may not be evident on CT or conventional bone scintigraphy alone. While the relationship of diffusion restriction with disease status is complex, ADC values and appearance on DWI, in conjunction with changes in FDG uptake, may be useful

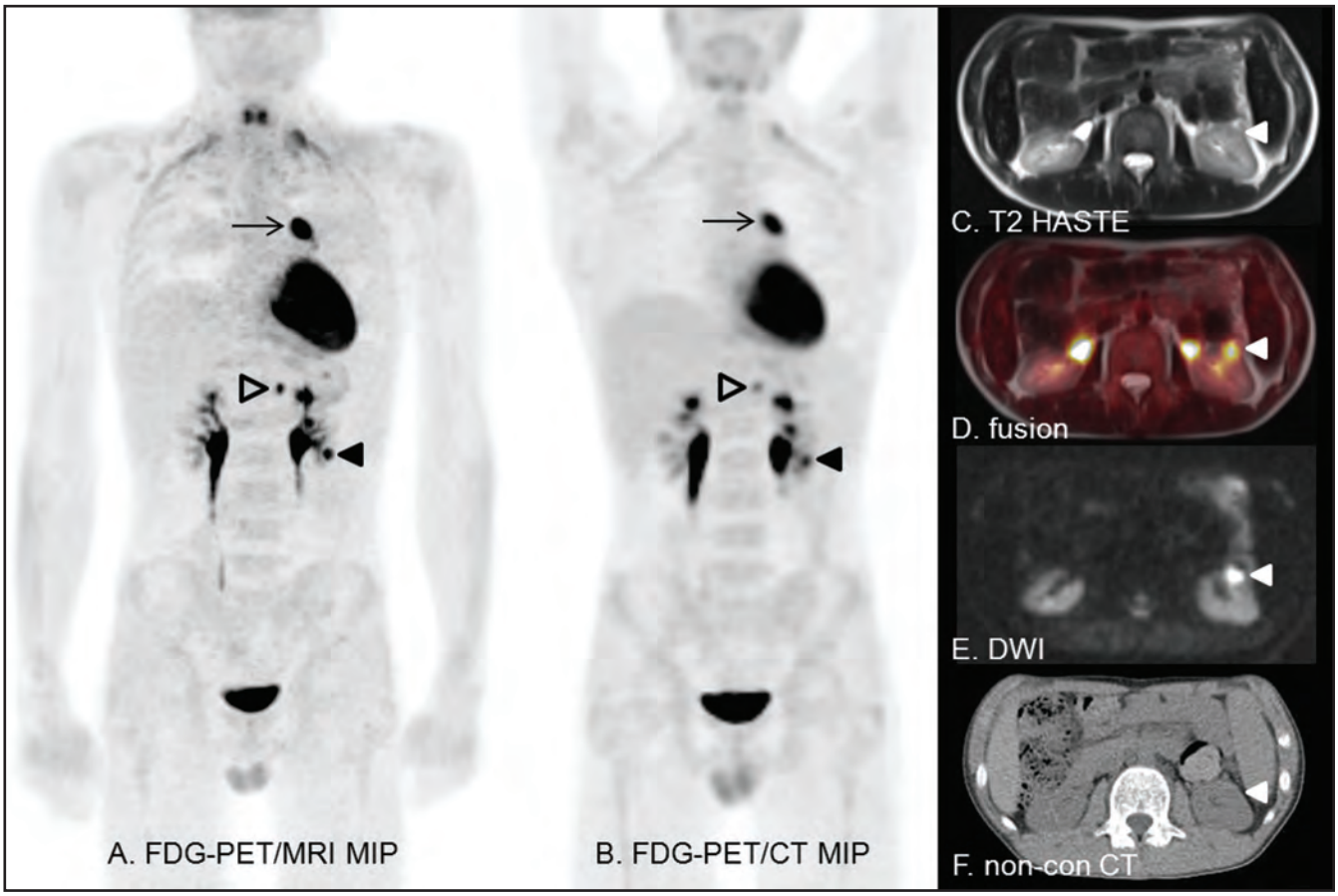

FIGURE 7. *B-cell lymphoma undergoing restaging after chemotherapy. Anterior PET/MRI (A) and PET/CT (B) maximal intensity projection (MIP) images show a hypermetabolic focus in the mediastinum (arrow), which was pathologically proven recurrent disease. A hypermetabolic lymph node (open arrow) is also suspicious for disease involvement. A third lesion in the left kidney (solid arrowhead) is difficult to differentiate from collecting system activity on the CT (F); however, axial HASTE (C), fused (D), and diffusion-weighted (E) MR images show that this represents a renal lesion.*

for monitoring response to therapy in neoplasms involving the bone.

Figure 4 consists of images of a 62-year-old woman with biopsy-proven multiple myeloma presenting for initial staging. A large, left humeral neck lesion is clearly depicted on DWI, ADC, and T2-inversion recovery, fat-suppressed MR sequences, with increased FDG uptake shown on the fused image. This lesion is less conspicuous on CT alone.

Cardiac imaging

Cardiac PET/MRI could play a role in both cardiac ischemia and cardiac viability assessment. Potential clinical protocols, playing on the strengths of both modalities, include stable chest pain assessment, performing cine MRI cardiac function assessment, N-13 ammonia or Rb-82 PET myocardial perfusion imaging, and delayed contrast-enhanced inversion-recovery infarct imaging in a single examination. Combined FDG and delayed contrast-enhanced inversion-recovery cardiac imaging permit co-localized, simultaneously acquired functional and anatomic viability assessment that, theoretically, could play a role in imaging-directed ventricular tachycardia radiofrequency ablation or direct biventricular pacing in dyssynchrony.

Figure 5 shows simultaneously acquired ECG-gated PET and delayed contrast-enhanced (DCE) cardiac MR images (simultaneous acquisition of MR 2-point Dixon also acquired for AC), allowing for precise fusion imaging. PET data were acquired in list mode, binned, and reconstructed into 3 phases. DCE MR images acquired in diastole are fused with diastolic PET data to create the center image. This patient has a normal heart.

Cervical and pelvic cancers

FDG-PET/CT and MRI are well established for staging and monitoring treatment response in patients with cervical cancer and other pelvic malignancies. PET data provide tumor volume estimation, allowing for accurate radiation therapy planning, as well as prognostic information related to progression-free survival.[4-7] High-resolution MRI provides exquisite soft-tissue detail for local staging and presurgical planning. The combination of metabolic information derived from FDG-PET with high-resolution MRI of the pelvis shows promise in both clinical management and potential research

opportunities in correlating functional MRI with tumor metabolism.

Given the complex anatomy of the pelvis, multiplanar and high-resolution T2 TSE are mainstay sequences. Using a 3-dimensional (3D) isotropic dataset, such as T2 SPACE, a single acquisition can yield high-resolution images with the option of infinite reformatting without loss of resolution. DWI provides improved conspicuity of lymph nodes, and ADC values for primary cervical malignancy have been correlated with standardized uptake values (SUVs) for FDG, permitting an additional noninvasive biomarker of disease response. Additionally, volumetric-interpolated breath-held examination (VIBE) can provide excellent anatomic detail of pelvic structures. Radial VIBE allows for a free-breathing acquisition with acceptable resolution and no motion artifact.

Figure 6 consists of images of a 58-year-old woman with newly diagnosed cervical cancer presenting for initial staging. Additional images from a separate patient who underwent total abdominal hysterectomy and bilateral salpingo-oophorectomy demonstrate the utility of T2-SPACE multiplanar reformats.

Pediatric imaging

PET/MRI is especially appealing in the pediatric population, as it is associated with less radiation exposure than PET/CT without compromising anatomic image quality. A recent study performed at the University of Leipzig in Germany showed that the effective dose of a PET/MRI scan is only about 20% that of the equivalent PET/CT examination. Children with systemic malignancies routinely evaluated with PET/CT (such as lymphoma) could benefit from the reduced radiation exposure of PET/MRI.

Simultaneously acquiring PET and MRI data combines the advantages of two previously separate advanced-imaging modalities, a tremendous advantage in young children requiring sedation/anesthesia for imaging. The improved soft-tissue contrast and molecular imaging (such as diffusion and perfusion imaging) abilities of MRI permit better detection of lymph-node and visceral disease than does CT. PET/MRI also holds great potential in evaluating soft-tissue malignancies, such as sarcomas, in the pediatric population.

Figure 7 presents the images of a 16-year-old boy with diffuse, large B-cell lymphoma undergoing restaging after chemotherapy. Excellent PET and MRI coregistration helps separate the renal lesion (solid arrowhead) from excreted FDG in the collecting system.

Conclusion

PET/MRI shows promise for multiple clinical applications through the combination of the improved soft-tissue contrast of MRI with lower radiation dose, and the potential for better correlation of PET findings to anatomy given the simultaneous acquisition. Several challenges are evident in developing optimal protocols, including optimal MR-sequence parameters, motion correction, and validation of the quantitative accuracy of PET with MRI-based attenuation correction. In some cases, the combination of SUVs measured on PET and ADC values measured on diffusion-weighted MRI may prove more specific than subjective assessment alone in differentiating tumor from surrounding tissue. The potential for benefit from PET/MRI acquisition also exists in receptor-targeted oncologic imaging, dementia assessment, and cardiac and atherosclerosis imaging.

Acknowledgements

We acknowledge the invaluable assistance of Jennifer Frye, Glenn Foster, Linda Becker, Debra Hewing, Michael Harrod, Tim Street, and Betsy Thomas.

References

1. Pichler BJ, Judenhofer MS, Wehrl HF. PET/MRI hybrid imaging: Devices and initial results. *Eur Radiol.* 2008;18:1077-1786.
2. Antoch G, Bockisch A. Combined PET/MRI: A new dimension in whole-body oncology imaging? *Eur J Nucl Med Mol Imaging.* 2009;36 Suppl 1:S113-20.
3. Wehrl HF, Sauter AW, Judenhofer MS, Pichler BJ. Combined PET/MR imaging--technology and applications. *Technol Cancer Res Treat.* 2010;9:5-20.
4. Buchbender C, Heusner TA, Lauenstein TC, et al. Oncologic PET/MRI, Part 1: Tumors of the brain, head and neck, chest, abdomen, and pelvis. *J Nucl Med.* 2012;53:928-938.
5. Buchbender C, Heusner TA, Lauenstein TC, et al. Oncologic PET/MRI, Part 2: Bone tumors, soft-tissue tumors, melanoma, lymphoma. *J Nucl Med.* 2012;53:1244-1252.
6. Drzezga A, Souvatzoglou M, Eiber M, et al. First clinical experience with integrated whole-body PET/MR: Comparison to PET/CT in patients with oncologic diagnoses. *J Nucl Med.* 2012;53: 845-855.
7. Martinez-Moller A, Eiber M, Nekolla S, et al. Workflow and scan protocol considerations for integrated whole-body PET/MRI in oncology. *J Nucl Med.* 2012;53:1415-1426.
8. Kidd EA, Siegel BA, Dehdashti F, Grigsby PW. The standardized uptake value for F-18 fluorodeoxyglucose is a sensitive predictive biomarker for cervical cancer treatment response and survival. *Cancer.* 2007;110:1738-1744.
9. Kidd EA, Grigsby PW. Intratumoral metabolic heterogeneity of cervical cancer. *Clin Cancer Res.* 2008; 14:5236-5241.
10. Schwarz JK, Siegel BA, Dehdashti F, Grigsby PW. Association of post-therapy positron emission tomography with tumor response and survival in cervical carcinoma. *JAMA.* 2007;298:2289-2295.
11. Olsen JR, Esthappan J, Dewees T, et al. Tumor volume and subvolume concordance between FDG-PET/CT and diffusion-weighted MRI for squamous cell carcinoma of the cervix. *J Magn Reson Imaging.* 2013; 37:431-434.
12. Hirsch FW, Sattler B, Sorge I, et al. PET/MR in children. Initial clinical experience in paediatric oncology using an integrated PET/MR scanner. *Pediatr Radiol.* 2013 Jan 11. [Epub ahead of print].